EasyChair Preprint

№ 12407

CFD Analysis of Hydrodynamic Journal Bearing Operating with Non-Newtonian Lubricant

Pranav Mehrotra, Paras Seth, Ishaan Nagpal, Devansh Rastogi and Vivek Kumar

March 6, 2024

CFD Analysis of Hydrodynamic Journal Bearing Operating with non-Newtonian Lubricant

[1]Pranav Mehrotra, [2]Paras Seth, [3]Ishaan Nagpal, [4]Devansh Rastogi, [5]Vivek Kumar
[1-5]Department of Mechanical Engineering, NSUT Dwarka, New Delhi
Email ID: [1]pranavm1002@gmail.com

Abstract

The hydrodynamic journal bearing is a crucial machine element used to support radial load in turbomachines. The research in journal bearings focuses on enhancing the steady state and dynamic performance indices. This study deals with the CFD simulations of hydrodynamic journal bearing operating with non-Newtonian lubricants. The CFD simulations have been performed using the Fluent module of Ansys 2023. The Power law fluid model has been used to describe the non-Newtonian character of the lubricant. The plots are generated for maximum fluid pressure, film pressure distribution, and turbulence dissipation for the Newtonian, pseudoplastic, and Dilatant nature of lubricant. Insights into fluid film pressure distribution and turbulence dissipation rates inform guiding designers for improved performance. Understanding maximum pressure trends is vital for design assessment, preventing failures, and optimizing the durability of the hydrodynamic journal bearings. Practical applications for machine designers include a comprehensive understanding of design parameters' impact on performance, ensuring reliability in turbomachines. Overall, the research contributes to the field, offering academic and simulation insights of a hydrodynamic journal bearing.

Keywords: *Hydrodynamic Journal Bearing, Computational Fluid Dynamics, Non-Newtonian Lubricant.*

1. Introduction

The research on hydrodynamic journal bearings is propelled by their capability to endure radial loads, especially in challenging operational conditions and environments where rolling element bearings prove to be ineffective [1]. These bearings rely on a thin lubricant film to support the external load acting on the journal bearing system. It is imperative to comprehend the pressure distribution and load-carrying capacity of these bearings for their design and performance optimization. The study of hydrodynamic journal bearings entails solving the compressible

Reynolds equation using numerical techniques such as the Finite Difference Method [2], Finite Element Method [3-5], Finite volume method [6], CFD [7-9], Modified Parabolic Approximation, etc. These approaches offer insights into the dynamic characteristics of these bearings and contribute to the design of advanced bearing systems [1-9].

Furthermore, the optimization of hydrodynamic journal bearings plays a crucial role in enhancing their performance and efficiency. Narwat et al [3,5] performed numerical simulations to investigate the effect of the number of lobes on the steady-state and dynamic performance indices of the hydrodynamic journal bearings. The authors recommended two-lobe journal bearing for better rotor dynamic performance from the journal bearing system. Wang et al. [6] performed a thermo-hydrodynamic analysis of combined journal and thrust bearing provided with herringbone grooves. Since the last decades, efforts have been made to enhance the load-carrying capacity and reduce the frictional power loss in fluid film bearings by altering the bearing geometry at micro-scales [9-14]. In this technique, well-defined micro-features in the form of grooves or dimples are provided on the bearing surfaces. It has been reported that these micro-features with optimum attributes can significantly improve the performance of hydrodynamic/hybrid journal [9-12], slider [13], and thrust bearings [14] considerably. The combined effect of slip boundary conditions and surface texture has been observed to enhance the tribological performance of hydrodynamic journal bearings [13].

The commercially available lubricants are often blended with additives to improve the viscosity and stability of oils under given operating conditions [1]. The presence of additives makes lubricating oil exhibit non-Newtonian character. The primary motivation for studying journal bearings operating with non-Newtonian lubricants is to generate more realistic data concerning the steady-state and dynamic performance parameters of the bearing. The use of non-Newtonian oils results in significant variations in the load-carrying capacity and friction power loss in actual operating conditions. Many studies [2,14-19] have been reported investigating the performance of fluid film bearing operating with non-Newtonian lubricant obeying the Rabinowitsch fluid model [2,15-16], Bingham model [17], Power law model [18], etc. The investigation into the influence of non-Newtonian pseudo-plastic lubricants [15] on the static characteristics of self-lubricating porous journal bearings with circular geometry is undertaken due to the potential impact of these fluids on load-carrying capacity and pressure distribution. Employing non-Newtonian lubricants can enhance the stability threshold speed margin and reduce frictional power loss, ultimately

improving the overall performance of the bearings [18]. Nowadays, bearing designers are using smart lubricants such as Electro-rheological lubricants [20-22] and Electrically conducting oils [23] to improve the steady-state and dynamic performance of fluid film bearings. These kinds of lubricants can adjust the viscosity of lubricant in real time by altering the magnitude of activating the electric/magnetic field. A marked improvement in load-carrying capacity and stiffness characteristics of fluid film bearing have been reported by the use of smart lubricants [20-25].

The literature review on hydrodynamic journal bearings suggests there is a dearth of studies dealing with CFD simulations of textured surface hydrodynamic journal bearings operating with non-Newtonian fluids. Because of this; this study has been planned to perform CFD analysis of hydrodynamic journal bearing operating with power law lubricant.

2. Governing Equations

The schematic of the hydrodynamic journal bearing under investigation is shown in Figure 1. Navier Stokes equation is used for the simulation of hydrodynamic journal bearing. The application of Navier-Stokes equations to non-Newtonian fluids is dependent on the fluid rheological behavior. Key considerations include the need for a constitutive model to characterize the relationship between stress and strain rate, accommodating variations in viscosity by expressing it as a function of shear rate or stress. Addressing non-Newtonian behaviors which include shear-thinning or viscoelasticity, recognizing that universality in applying Navier-Stokes equations may not hold for all non-Newtonian fluids, and recognizing the need for rheological measurements to determine viscosity. Furthermore, empirical correlations established from experimental data could offer beneficial data on the stress-strain rate relationship in non-Newtonian fluids.

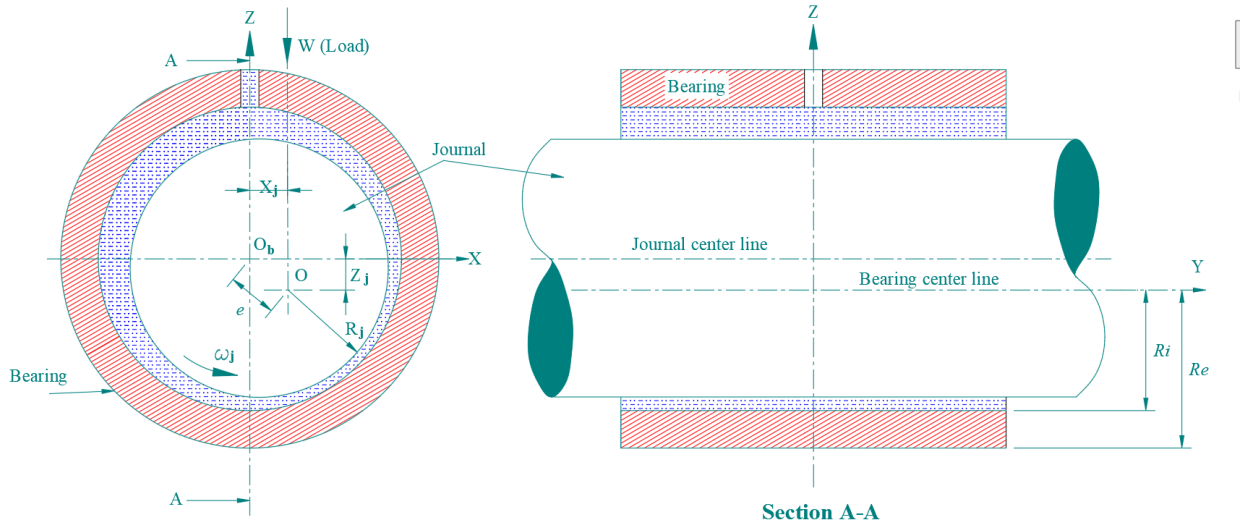

Figure. 1: Schematic of a Hydrodynamic Journal Bearing

The flow governing equation used for the analysis of hydrodynamic journal bearings are as follows [1]:

Continuity Equation:

$$\frac{\partial \rho}{\partial t} + \frac{\partial (\rho u)}{\partial x} + \frac{\partial (\rho v)}{\partial y} + \frac{\partial (\rho w)}{\partial z} = 0 \tag{1}$$

Conservation of Momentum along the X axis:

$$\frac{\partial (\rho u)}{\partial t} + \frac{\partial (\rho u^2)}{\partial x} + \frac{\partial (\rho uv)}{\partial y} + \frac{\partial (\rho uw)}{\partial z} = -\frac{\partial p}{\partial x} + \frac{1}{Re_r}\left[\frac{\partial \tau_{xx}}{\partial x} + \frac{\partial \tau_{xy}}{\partial y} + \frac{\partial \tau_{xz}}{\partial z}\right] \tag{2}$$

Conservation of momentum along the Y axis:

$$\frac{\partial (\rho v)}{\partial t} + \frac{\partial (\rho uv)}{\partial x} + \frac{\partial (\rho v^2)}{\partial y} + \frac{\partial (\rho vw)}{\partial z} = -\frac{\partial p}{\partial y} + \frac{1}{Re_f}\left[\frac{\partial \tau_{xy}}{\partial x} + \frac{\partial \tau_{yy}}{\partial y} + \frac{\partial \tau_{yz}}{\partial z}\right] \tag{3}$$

Conservation of Momentum along the Z axis:

$$\frac{\partial (\rho w)}{\partial t} + \frac{\partial (\rho uw)}{\partial x} + \frac{\partial (\rho vw)}{\partial y} + \frac{\partial (\rho w^2)}{\partial z} = -\frac{\partial p}{\partial z} + \frac{1}{Re_r}\left[\frac{\partial \tau_{xz}}{\partial x} + \frac{\partial \tau_{yz}}{\partial y} + \frac{\partial \tau_{zz}}{\partial z}\right] \tag{4}$$

Conservation of Energy:

$$\frac{\partial (E_T)}{\partial t} + \frac{\partial (uE_T)}{\partial x} + \frac{\partial (vE_T)}{\partial y} + \frac{\partial (wE_T)}{\partial z}$$

$$= -\frac{\partial (up)}{\partial x} - \frac{\partial (vp)}{\partial y} - \frac{\partial (wp)}{\partial z} - \frac{1}{Re_r Pr_r}\left[\frac{\partial q_x}{\partial x} + \frac{\partial q_y}{\partial y} + \frac{\partial q_z}{\partial z}\right]$$

$$+ \frac{1}{Re_r}\left[\frac{\partial}{\partial x}\left(u\tau_{xx} + v\tau_{xy} + w\tau_{xz}\right) + \frac{\partial}{\partial y}\left(u\tau_{xy} + v\tau_{yy} + v\tau_{yz}\right) + \frac{\partial}{\partial z}\left(u\tau_{xz} + v\tau_{yz} + w\tau_{zz}\right)\right]$$

(5)

3. Solution Procedure

3.1 Lubricant Film Modelling

A CAD model of the lubricant film (Fig.2) is created using the parameters given in Table 1. The different configuration of the model is recreated for all the required values of the eccentricity ratio (0.5~0.9).

Table 1: Cad Modelling Parameters [12]

Parameter	Dimensional Value
Journal radius	25 mm
Bearing Inner radius	25.2 mm
Bearing outer radius	29 mm
Length of bearing	50 mm
Eccentricity ratio	0.5-0.8
Radial Clearance	50 μm

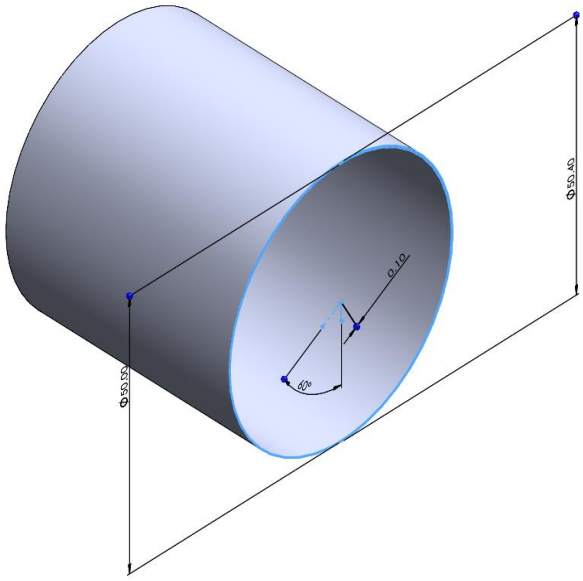

Figure 2: Oil Film CAD Model

3.2 Defining Material properties

Hydrodynamic journal bearings generally use NLGI 3 oil for lubrication [24]. NLGI 3 is a thick oil which is recommended for high load commercial usage. NLGI 3 oil of all brands were surveyed

and on the basis of the survey conducted, the material properties of the lubricant, as listed in table 2 were chalked out.

Table 2: Lubricant Properties [25]

Property	Value
Consistency Index(k)	0.05 (kg s^{-2} m^{-1})
Thickener percentage	16.5%
Power Law Index(n)	0.8;1.0;1.2
Minimum Viscosity	0.012 (kg/ms)
Maximum Viscosity	0.174 (kg/ms)

The value of the power law index depends on the concentration of the thickening agent polyacrylamide [25]. The power factor was determined using a graph in Figure. 3.

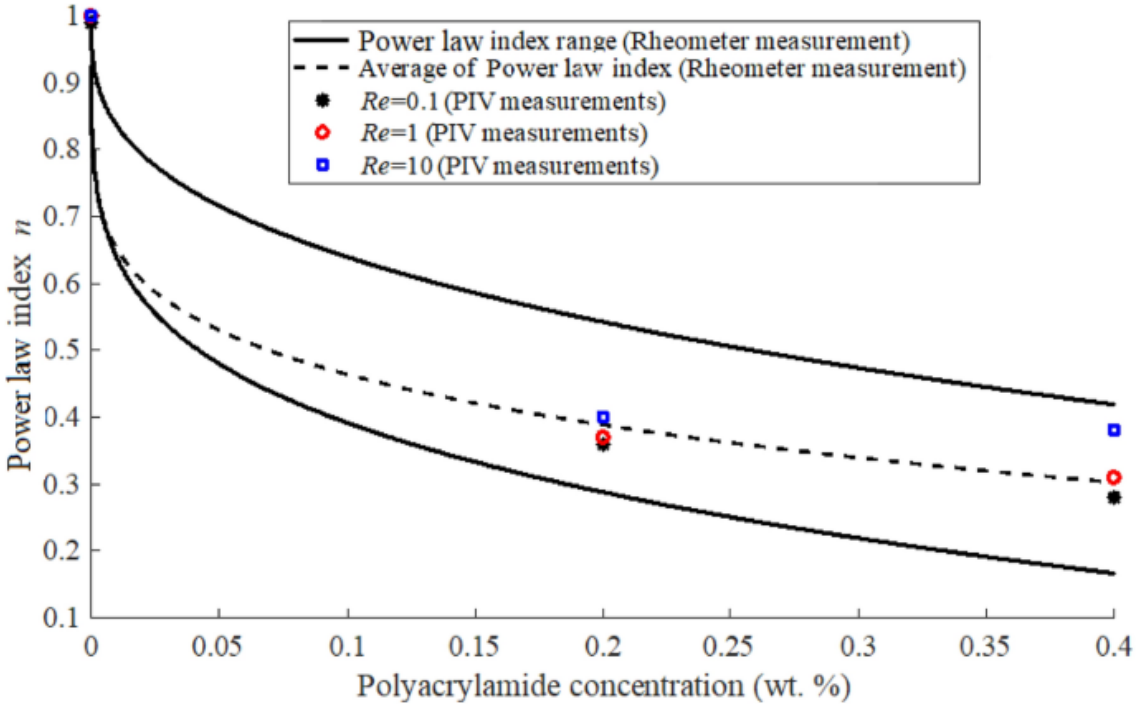

Figure. 3: Polyacrylamide concentration vs power law index [25]

3.3 Discretization of Flow Domain

The CAD model created previously is imported into Ansys fluent module. The model must be meshed for analysis to take place. Following steps have been used for performing meshing of the flow domain,

1. Select the left side annular surface and create a named selection *INLET*. Similarly, select the right side annular surface and create a named selection *OUTLET*.
2. Select The outer wall and create a name selection *Stationary Wall*.
3. Select the inner wall and create a name selection *Rotating Wall*.
4. Create a coordinate system with the inner wall as the point of reference and note down the coordinates of origin.
5. Insert a body sizing in the mesh tab and define the required element size.
6. Turn on adaptive mesh size and increase mesh smoothing to the highest level.
7. Generate the mesh (Fig.4).

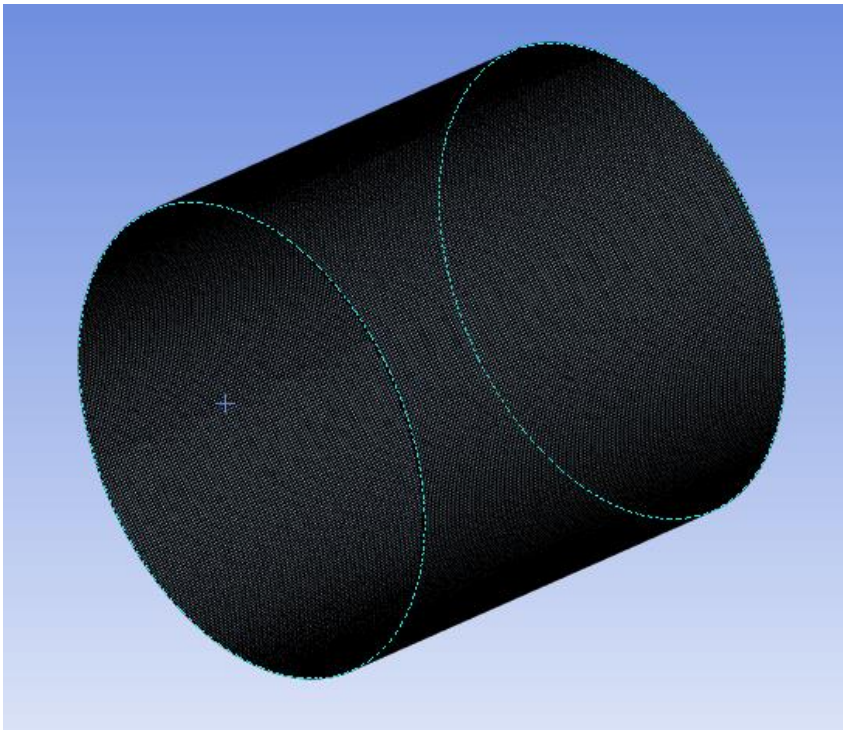

Figure. 4: Discretization of fluid flow domain

The grid independence test has been conducted to obtain the minimum number of elements required to perform CFD simulation of journal bearing. Table 3 depicts the variations in maximum

pressure with successive increases in the number of elements. After a certain mesh size, the numerical results tend to converge and the output becomes nearly constant (less than 1% variation). At an element size of 0.5 mm, the numerical results become independent of the grid size and any further increase in the mesh elements would exponentially increase the computation time without a noticeable effect on the accuracy results. Hence a mesh size of 0.5 mm is adopted to save computation cost in numerical simulations.

Table 3: Data for Grid Independence Test

Element Size	P max (Pa)	Percent change
10.00	1144068.00	
9.00	148227.30	-671.83%
8.00	124542.10	-19.02%
7.00	104689.20	-18.96%
6.00	293963.00	64.39%
5.00	1044375.00	71.85%
4.00	861085.90	-21.29%
3.00	823426.80	-4.57%
2.00	993610.00	17.13%
1.00	1050711.00	5.43%
0.95	1236935.00	15.06%
0.90	1141987.00	-8.31%
0.85	1177925.00	3.05%
0.80	1084999.00	-8.56%
0.75	1053463.00	-2.99%
0.70	1045997.00	-0.71%
0.65	1089095.00	3.96%
0.60	1107924.00	1.70%
0.55	1103103.00	-0.44%
0.50	1106528.00	0.31%
0.45	1112652.00	0.55%
0.40	1123319.00	0.95%

3.4 Simulation Setup

Following steps have been used to perform CFD simulation of hydrodynamic journal bearing using Fluent module of Ansys 2021.

1. Start the simulation setup and select a double precision solver and select the number of parallel machines.
2. Check for negative minimum volume.
3. Turn on the multiphase mixture model.
4. Select the k epsilon 2 equation viscosity model
5. Set the boundary conditions.
6. Define pressure at the inlet and outlet boundary.
7. Define the boundary condition of the inner wall as a rotating wall, and enter coordinates of the rotation axis and rpm.
8. To initialize non-Newtonian behavior, write the commands shown in Figure. 2.5 in the terminal.

```
> define

/define> model

/define/models> viscous

/define/models/viscous> turbulence-expert

/define/models/viscous/turbulence-expert> turb-non-newtonian
Enable turbulence for non-Newtonian fluids? [yes] yes
```

Figure. 5: Initialization of non-Newtonian behavior

9. To define material properties, select non-Newtonian power law as the viscosity model, and fill out the properties determined in section 3.2.
10. Set residual convergence to 10^{-6}.
11. Initialize the solutions using hybrid mode
12. Set up the solution iterations and define the time step.
13. Run the solutions.

14. Check the scaled residual graph for convergence (Figure 6). If convergence is achieved, then we can study the contours as per our requirement.

The residual convergence test has been performed to get the minimum number of iterations required to yield converged results for primary variables in an iterative solution scheme. In the convergence test, the difference in primary variables between successive iterations, is known as residuals. It is performed to see if the solution is approaching towards a stable state. A decreasing residual shows convergence, which means that successive iterations result in smaller changes and the solution is approaching convergence. It can be seen from Figure 6 that the residuals converge after 50 iterations. In iterative algorithms, this test is critical for assuring computational efficiency and dependability and it gives us a minimum number of iterations necessary to reach a stable solution.

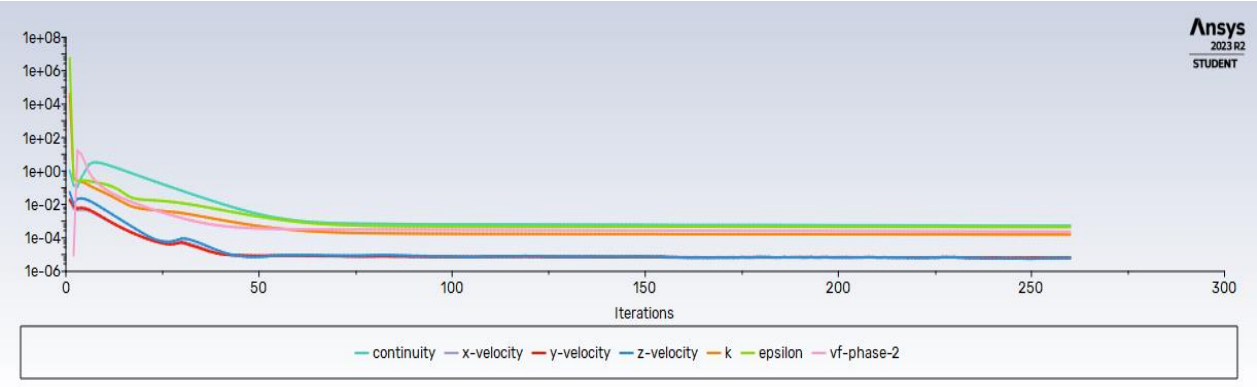

Figure. 6: Residual convergence

3.5 Validation of the proposed model

The developed model based on CFD simulation has been validated with published results [26] on hydrodynamic journal bearing. This is required to check the adequacy of the developed model to generate accurate numerical results for the bearing system. Maneshian and Nassab [26] performed CFD simulations on hydrodynamic journal bearing operating under turbulent conditions. Figure 7 presents a comparison of maximum pressure values vs eccentricity ratio in the reference study [26] and developed model under identical geometric and operating conditions. It can be seen that trends of maximum pressure vs eccentricity ratio from the two studies are closely following each other.

This justifies the adequacy of the developed CFD model to simulate a hydrodynamic journal-bearing system.

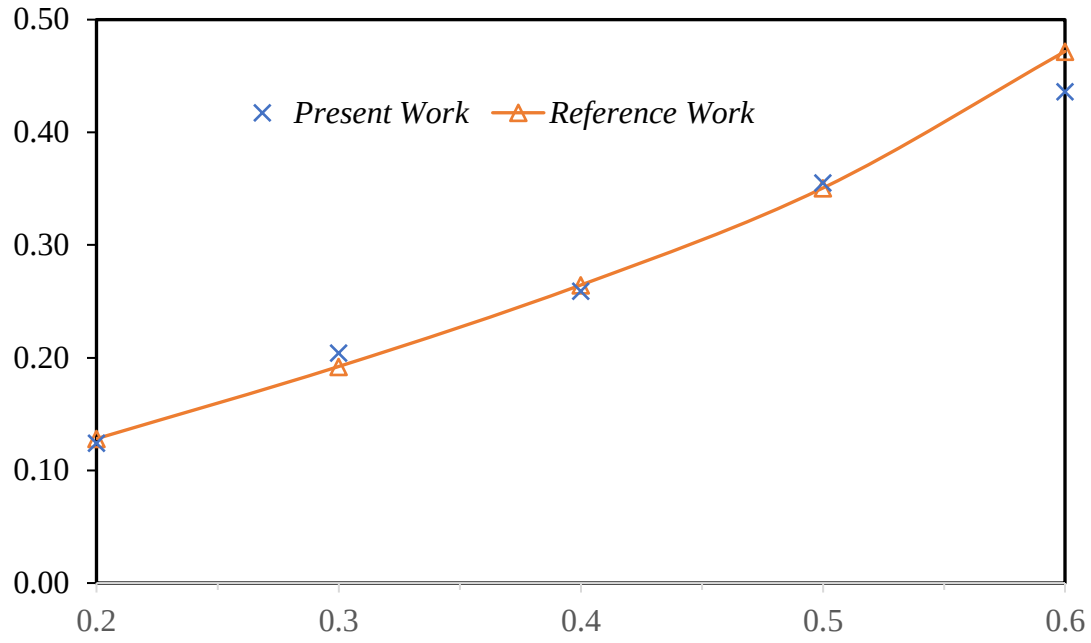

Figure. 7: Maximum pressure vs Eccentricity ratio [26]

4. Results and Discussions

In this section, the effect of the non-Newtonian nature of lubricant has been discussed on fluid film pressure, load carrying capacity, and turbulence dissipation rate in a hydrodynamic journal bearing. The non-Newtonian lubricant follows the power law model to describe shear stress as a function of strain rate. For a power index less (n) than one, the fluid exhibits pseudo-plastic or shear thinning behavior. For Power equal to one, it follows the Newtonian behavior, and for a power index greater than one the lubricant is dilatant or shear thickening. The CFD analysis for lubricant was carried out for n=0.8, n=1, and n= 1.2 keeping bearing geometric and operating conditions identical. The behavior of the three types of lubricant fluids was observed for the fluid film pressure profile as depicted in Figure 8-10. It can be seen from Figure 8-10, that use of Dilatant lubricant vis-à-vis Newtonian and Pseudoplastic lubricant generates a higher value of maximum hydrodynamic

pressure. Further, it can be seen that Dilatant lubricant generates better hydrodynamic action (larger higher pressure zone). It could be due to the higher apparent viscosity exhibited by dilatant lubricant during the shearing of the lubricating film.

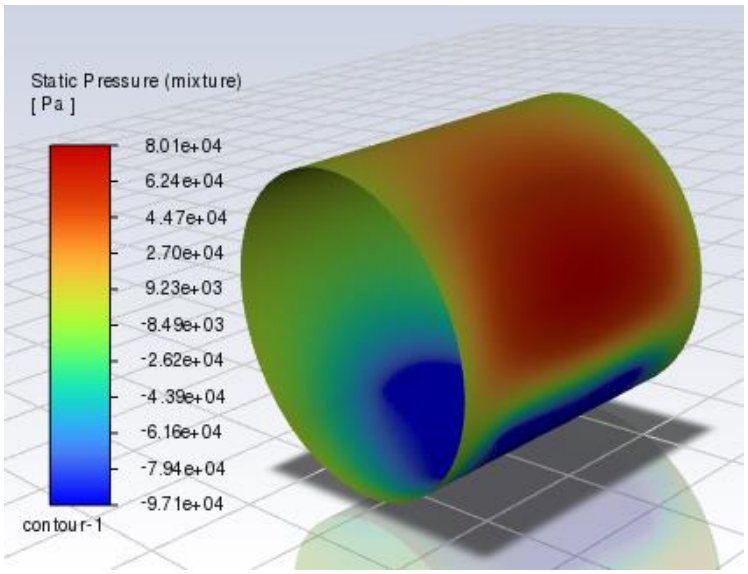

Figure. 8: Pressure Contour of Journal Bearing operating with Dilatant lubricant (n=1.2)

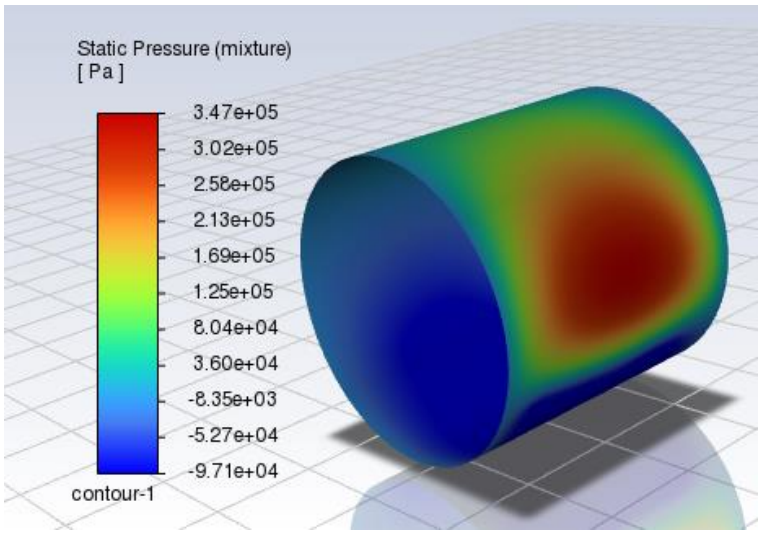

Figure. 9: Pressure Contour of Journal Bearing operating with Newtonian fluid (n=1)

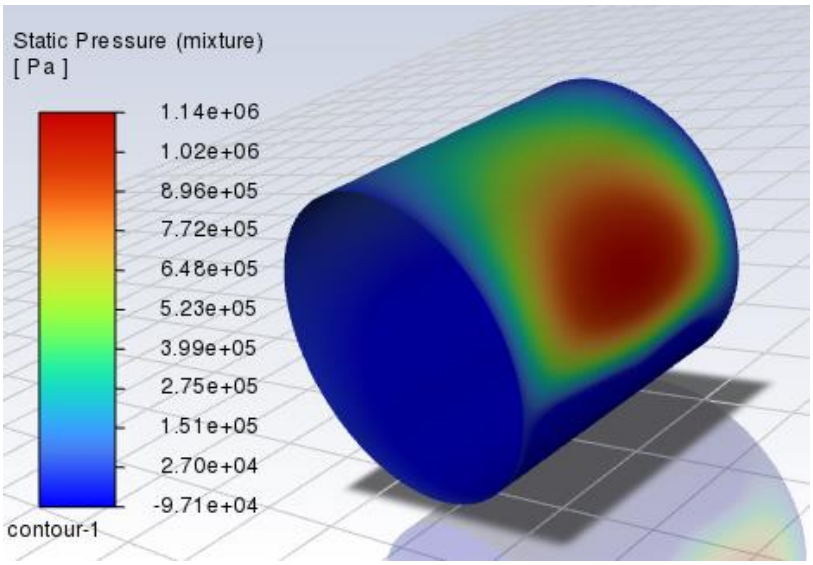

Figure. 10: Pressure Contour of Journal Bearing operating with Pseudoplastic Lubricant (n=0.8)

The presence of inherent eccentricity in the centers of the journal and shaft results in the formation of a thin lubricant film with non-uniform thickness. The creates a converging-diverging passage to be thinner on one side and thicker on the opposite side. As a result, hydrodynamic action will build up, which leads to a variation in the fluid pressure in the lubricant.

Upon examination of the pressure contours produced through the utilization of computational fluid dynamics (CFD) analysis, it was noted that the highest level of fluid pressure is situated near the region with the smallest fluid film thickness. Additionally, the encompassing areas exhibit a gradual escalation in pressure as they approach the zone of minimal film thickness. This particular region characterized by the increasing pressure is commonly referred to as the "convergent zone". The trends depicted in the illustration (Figure 11) indicate that as the eccentricity ratio rises, so does the pressure. This phenomenon is a result of the film becoming thinner at the location of minimal thickness, leading to a highly converging passage for the circulating oil and a subsequent enhancement in the maximum hydrodynamic pressure exerted by the lubricating film.

When examining the dilatant, Newtonian, and pseudo-plastic behavior of lubricant, it becomes apparent that the dilatant lubricant exhibits the highest maximum film pressure, while the pseudo-plastic fluids display the lowest maximum film pressure. This phenomenon arises from the escalating viscosity of dilatant fluids, which intensifies with hydrodynamic action in the film, thereby inducing higher maximum film pressures. Conversely, the viscosity of pseudo-plastic fluids diminishes, leading to lower maximum film pressures.

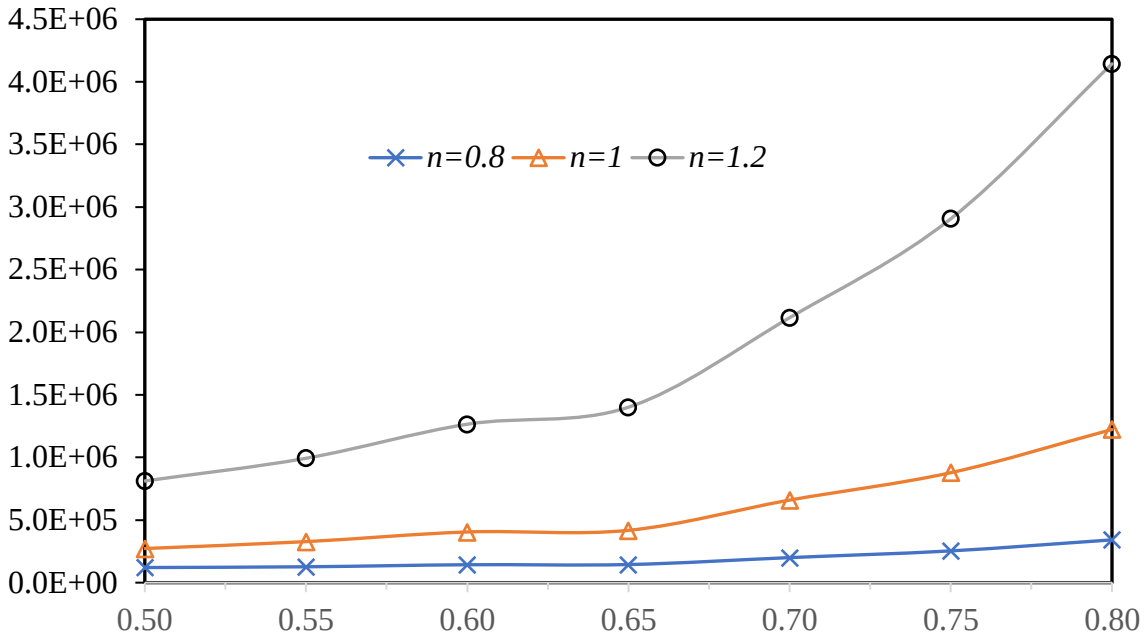

Figure. 11: Maximum pressure (Pa) vs eccentricity ratio

The dissipation rate of turbulence is a measure of how quickly turbulent energy is converted into heat through viscous forces. In the context of fluid dynamics, turbulence dissipation rate is often denoted by the symbol ε (epsilon). When it comes to estimating power loss in a turbulent flow, the dissipation rate plays a role in determining the rate at which kinetic energy is converted into internal energy, primarily through viscous dissipation. The trends in the Figure 12 show that the turbulence dissipation rate increases with increasing eccentricity ratio. This occurs because the cavitation and heating occur more rapidly when the film gets thinner at a point. On comparing dilatant, pseudoplastic, and Newtonian lubricant, it is found that dilatant lubricant dissipates the most energy whereas pseudoplastic lubricants dissipates the least at lower eccentricity ratios. Higher eccentricity ratios, on the other hand, cause the pattern to invert, with dilatant lubricants showing lower dissipation rates and pseudoplastic lubricants showing greater rates of dissipation.

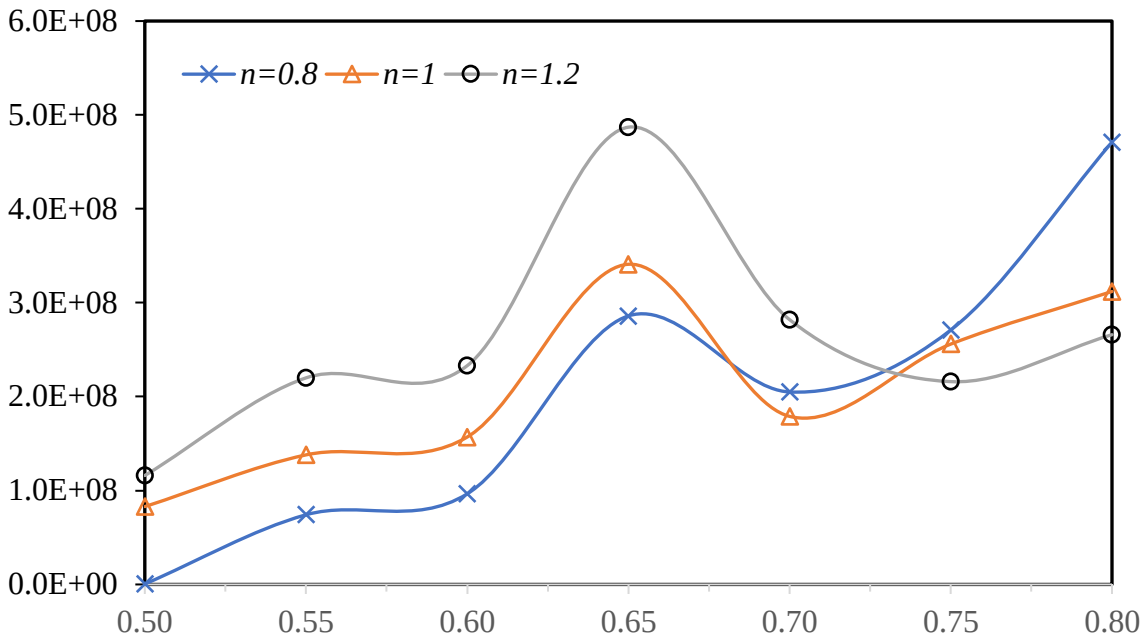

Figure 12: Turbulence dissipation rate vs eccentricity ratio

In journal bearings, the load-carrying capacity serves as a metric to assess the bearing's efficacy in accommodating and dispersing the loads imposed upon it during operation. The bearing's capacity to provide support to rotating machinery and prevent any direct contact between the journal and the bearing surface hinges primarily upon this capability. It denotes the maximum force that can be exerted upon the bearing without rupturing the fluid. The disruption of the fluid film results in the contact of the shaft and the journal, thereby engendering heightened levels of heating and vibrations, consequently leading to diminished efficiency and posing a potential hazard to safety. The trends in the Figure 13 show that load-carrying capacity increases with increasing eccentricity ratio. This occurs due to the higher film pressure experienced by the bearing at higher eccentricity ratios. Upon comparison of Dilatant, pseudoplastic, and Newtonian lubricants, it is observed that dilatant lubricants offer the highest load-carrying capacity under the same operating conditions. These trends are in line with the maximum film pressures observed for three types of lubricants (Figure 8-11).

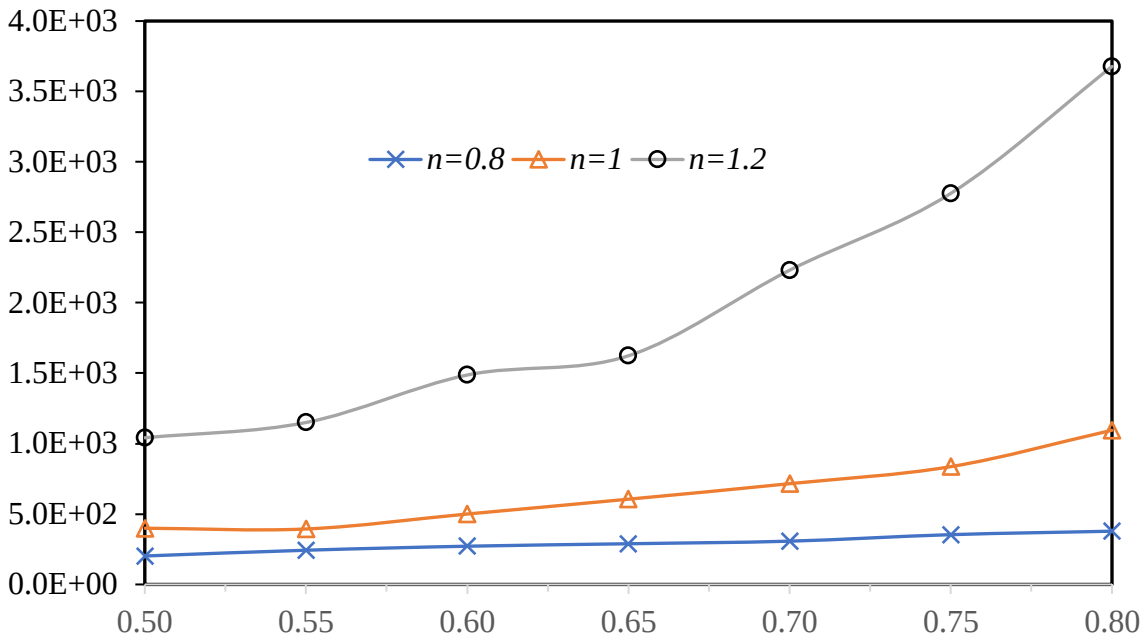

Figure 13: Load Carrying Capacity (N) vs eccentricity ratio

5. Conclusions

Following major conclusions can be drawn from the CFD analysis of journal bearing done in this study,

- The dilatant lubricant generates higher value of maximum film pressure and bigger higher pressure zone vis a vis Pseudoplastic lubricant.
- The energy dissipation rate increases with an increase in eccentricity ratio. The dilatant lubricant generates a higher energy dissipation rate (frictional power loss) in the bearings.
- Dilatant lubricant vis-à-vis Pseudoplastic lubricant significantly enhances the load-carrying capacity of the journal bearing.

References

[1] Bhushan, Bharat. *Introduction to tribology*. John Wiley & Sons, 2013.

[2] Boubendir, S., S. Larbi, M. Malki, and R. Bennacer. "Hydrodynamic self-lubricating journal bearings analysis using Rabinowitsch fluid lubricant." *Tribology International* 140 (2019): 105856.

[3] Narwat, Kuldeep, Vivek Kumar, Simran Jeet Singh, Abhishek Kumar, and Satish C. Sharma. "Performance of rough surface hydrodynamic circular and multi-lobe journal bearings in turbulent regimes." Proceedings of the Institution of Mechanical Engineers, Part J: Journal of Engineering Tribology 237, no. 4 (2023): 860-880.

[4] Singh, Saurabh, and Mohd Zaheen Khan. "Analysis of hydrodynamic compliant journal bearings." Materials Today: Proceedings 46 (2021): 6650-6654.

[5] Kumar, Vivek, Kush Shrivastava, Kuldeep Narwat, and Satish C. Sharma. "Influence of Number of Lobe on Dynamic Performance of Hydrodynamic Journal Bearing." In Advances in Mechanical and Materials Technology: Select Proceedings of EMSME 2020, pp. 211-224. Springer Singapore, 2022.

[6] Wang, Chin-Cheng, and Jyun-Ting Lin. "Numerical study of hydrodynamic herringbone-grooved journal bearings combined with thrust bearings considering thermal effects." Journal of Mechanics 38 (2022): 13-21.

[7] Dhande, D. Y., and D. W. Pande. "Multiphase flow analysis of hydrodynamic journal bearing using CFD coupled fluid structure interaction considering cavitation." Journal of King Saud University-Engineering Sciences 30, no. 4 (2018): 345-354.

[8] Tauviqirrahman, Mohammad, J. Jamari, Arjuno Aryo Wicaksono, M. Muchammad, S. Susilowati, Yustina Ngatilah, and Caecilia Pujiastuti. "CFD analysis of journal bearing with a heterogeneous rough/smooth surface." Lubricants 9, no. 9 (2021): 88.

[9] Nie, Tao, Kun Yang, Lei Zhou, Xin Wu, and Yin Wang. "CFD analysis of load capacity of journal bearing with surface texture." Energy Reports 8 (2022): 327-334.

[10] Shinde, Anil B., and Prashant M. Pawar. "Multi-objective optimization of surface textured journal bearing by Taguchi based Grey relational analysis." *Tribology International* 114 (2017): 349-357.

[11] Meng, Fanming, Yifei Zhang, Linlin Su, Haiyang Yu, and Yong Zheng. "Dynamic characteristics of compound textured journal bearing." *Proceedings of the Institution of Mechanical Engineers, Part J: Journal of Engineering Tribology* 235, no. 7 (2021): 1312-1334.

[12] Arif, M., Kango, S. and Shukla, D.K., 2022. Analysis of textured journal bearing with slip boundary condition and pseudoplastic lubricants. *International Journal of Mechanical Sciences*, *228*, p.107458.

[13] Rao, T. V. V. L. N., A. M. A. Rani, T. Nagarajan, and F. M. Hashim. "Analysis of slider and journal bearing using partially textured slip surface." *Tribology International* 56 (2012): 121-128.

[14] Kumar, Vivek, Satish C. Sharma, and Kuldeep Narwat. "Influence of micro-groove attributes on frictional power loss and load-carrying capacity of hybrid thrust bearing." *Industrial Lubrication and Tribology* 72, no. 5 (2020): 589-598.

[15] Sharma, Satish C., and Anil Singh. "A study of double layer conical porous hybrid journal bearing operated with non-Newtonian lubricant." *Tribology International* 179 (2023): 108183.

[16] Kumar, Vivek, Vatsalkumar Ashokkumar Shah, Kuldeep Narwat, and Satish C. Sharma. "Squeeze Film Operation of Thrust Bearing Operating with Shear-Thinning Lubricants." In Advances in Mechanical and Materials Technology: Select Proceedings of EMSME 2020, pp. 103-114. Springer Singapore, 2022.

[17] Silva, Fabrício Vieira, Maurício Araújo Zanardi, and Teófilo Miguel de Souza. "Analytical–numerical modeling of journal bearings with non-Newtonian fluids and cavitation effects." *Journal of the Brazilian Society of Mechanical Sciences and Engineering* 43 (2021): 1-16.

[18] Chetti, Boualem, Mohamed Hemis, Othman Tahar, and Moussa Smara. "Combined effects of elastic deformation and piezo-viscous dependency on the performance of a journal bearing operating with a non-Newtonian fluid." *Proceedings of the Institution of Mechanical Engineers, Part J: Journal of Engineering Tribology* 236, no. 12 (2022): 2457-2467.

[19] Narwat, Kuldeep, Vivek Kumar, Simran Jeet Singh, and Abhishek Kumar. "Performance analysis of circular and lemon bore hydrodynamic journal bearing considering surface roughness and shear thinning effect." In Aerospace and Associated Technology, pp. 101-105. Routledge, 2022.

[20] Singh, Atul Kumar, Vivek Kumar, Simran Jeet Singh, and Satish C. Sharma. "Performance of hybrid thrust bearing textured surface operating with electro-rheological lubricant." Proceedings of the Institution of Mechanical Engineers, Part J: Journal of Engineering Tribology 237, no. 4 (2023): 911-925.

[21] Singh, Atul Kumar, Vivek Kumar, Simran Jeet Singh, Naveen Sharma, and Divya Choudhary. "A comparative performance assessment of hydrostatic thrust bearings operating with electrorheological lubricant." Industrial Lubrication and Tribology 74, no. 7 (2022): 892-900.

[22] Gertzos, K. P., P. G. Nikolakopoulos, and C. A. Papadopoulos. "CFD analysis of journal bearing hydrodynamic lubrication by Bingham lubricant." Tribology international 41, no. 12 (2008): 1190-1204.

[23] Kumar, Vivek, Vatsalkumar Ashokkumar Shah, Simran Jeet Singh, Kuldeep Narwat, and Satish C. Sharma. "Rotor-dynamic performance of porous hydrostatic thrust bearing operating under magnetic field." Industrial Lubrication and Tribology 73, no. 2 (2021): 350-357.

[24] SKF.https://www.skf.com/in/products/super-precision-bearings/principles/bearing-selection-process/lubrication/suitable-grease. Accessed 6 Dec. 2023.

[25] NLGI-3 grease product sheet, https://www.tech-masters.com/en/download/6019

[26] Maneshian B, Nassab SAG, 2009, “Thermohydrodynamic analysis of turbulent flow in journal bearings running under different steady conditions”, Proc. IMechE Vol. 223 Part J: J. Engineering Tribology, v 223(8), pp 1115-1127.